Journal of Environmental Science International
30(1); 57~67; January 2021

pISSN: 1225-4517 eISSN: 2287-3503
https://doi.org/10.5322/JESI.2021.30.1.57

ORIGINAL ARTICLE

Application of Cu-loaded One-dimensional TiO_2 Nanorods for Elevated Photocatalytic Environmental Friendly Hydrogen Production

Dong Jin Kim*, Surendar Tonda, Wan-Kuen Jo

Department of Environmental Engineering, Kyungpook National University, Daegu 41566, Korea

Abstract

Photocatalytic green energy H_2 production utilizing inexhaustible solar energy has been considered as a potential solution to problems of energy scarcity and environmental contamination. However, the design of a cost-effective photocatalyst using simple synthesis methodology is still a grand challenge. Herein, a low-cost transition metal, Cu-loaded one-dimensional TiO_2 nanorods (Cu/TNR) were fabricated using an easy-to-use synthesis methodology for significant H_2 production under simulated solar light. X-ray photoelectron spectral studies and electron microscopy measurements provide evidence to support the successful formation of the Cu/TNR catalyst under our experimental conditions. UV-vis DRS studies further demonstrate that introducing Cu on the surface of TNR substantially increases light absorption in the visible range. Notably, the Cu/TNR catalyst with optimum Cu content, achieved a remarkable H_2 production with a yield of 39,239 μmol/g after 3 h of solar light illumination, representing 7.4- and 27.7-fold enhancements against TNR and commercial P25, respectively. The notably improved H_2 evolution activity of the target Cu/TNR catalyst was primarily attributed to its excellent separation and efficiently hampered recombination of photoexcited electron-hole pairs. The Cu/TNR catalyst is, therefore, a potential candidate for photocatalytic green energy applications.

Key words : Green energy, One-dimensional photocatalyst, Solar light, Cost effective, Optimum Cu

1. Introduction

Massive consumption of non-renewable fossil fuels for global energy demands results in scarcity of energy resources and environmental pollution. Therefore, the primary objective is to seek viable solutions that exclude the issues as mentioned above (Jo et al., 2018a; Jo et al., 2020). Solar-indued photocatalytic water reduction for the generation of clean hydrogen energy has been considered as a sustainable solution to rising energy shortages and environmental problems (Yuan et al., 2018; Ganguly et al., 2019; Kumaravel et al., 2019). In 1972, Fujishima and Honda discovered the photoelectrochemical production of hydrogen from water using the Pt/TiO_2 system. Since then, TiO_2-based materials are considered an attractive materials for a wide range of photocatalytic applications, including oxidation of organic compounds (Jo et al., 2018b; Li et al., 2019b), hydrogen production from water splitting (Zhang et al., 2017; Peng et al., 2018), and hydrocarbons generation from CO_2 reduction reaction (Sorcar et al., 2018; Sorcar et al., 2019), owing to their chemical

Received 23 November, 2020; **Revised** 14 December, 2020;
Accepted 14 December, 2020
***Corresponding author**: Dong Jin Kim, Department of Environmental Engineering, Kyungpook National University, Daegu 41566, Korea
Phone: +82-53-950-6584
E-Mail: eastcamp@knu.ac.kr

stability, non-toxicity, and high reactivity (Singh and Dutta, 2018). However, the optical response of TiO_2 is confined to the ultraviolet portion of the solar spectrum, resulting in limited utilization of solar energy (Khatun et al., 2018). Besides, TiO_2 is often known for its low quantum efficiency in photocatalytic applications because of the high recombination rate of photoexcited electron-hole pairs (Gao et al., 2019). Therefore, overcoming these disadvantages may present new directions to elevate the photocatalytic efficiency of TiO_2.

Tailoring TiO_2 could enhance its efficiency in the production of H_2 and give access to its intrinsic benefits. Several approaches have already been investigated to address the limitations of TiO_2, including loading noble or transition metals (Sharma and Lee, 2017; Wei et al., 2019), doping with foreign elements (Koltsakidou et al., 2017; Seetharaman et al., 2017), and forming composites by coupling TiO_2 with other semiconductors (Kim and Jo, 2018; Park et al., 2020). Among these approaches, loading TiO_2 with transition metals such as Cu, Fe, Ni, and Co could effectively improve the efficiency of TiO_2 by preventing recombination of electrons and holes through extracting generated electrons and improving visible light absorption (Jin and Jo, 2018). Cu is one of the cheapest and most promising transition metals that can be applied effectively to produce hydrogen (Lee et al., 2019). As such, the combination of TiO_2 and Cu metal is anticipated to have a synergistic impact on the photocatalytic efficiency of renewable H_2 production. Another approach to further improve the photocatalytic performance of TiO_2 is to tune its morphology. For instance, Jiang et al., (Jiang et al., 2018b) have demonstrated that the nanorod morphology of TiO_2 significantly boosts the photocatalytic evolution of H_2 compared to its TiO_2 counterpart with nanoparticle morphology. Moreover, TiO_2 nanorods may be of considerable value since they demonstrate a lower rate of recombination of photogenerated charges (Hu et al., 2019).

In view of the above factors, we rationally prepared a hybrid photocatalyst consisting of one-dimensional TiO_2 nanorods and low-cost Cu metal, using an easy synthesis route that includes hydrothermal and photodeposition methods. The fabricated Cu/TNR catalyst was thoroughly characterized by a variety of analytical tools. The photocatalytic performance of the Cu/TNR was assessed by recording the H_2 evolution under simulated sunlight illumination. The role of Cu content in the production of H_2 was carefully investigated. A plausible photocatalytic mechanism was also proposed based on the experimental studies.

2. Materials and Methods

2.1. Synthesis of TiO_2 Nanorods (TNR)

1.0 g of bare TiO_2 (P25, Evonik) was mixed with 30 mL of 10 N NaOH solution, transferred to a Teflon-lined autoclave and then thermally treated to 130℃ for 72 h in an oven. After cooling to room temperature, the white gel suspension obtained was washed with HCl (0.1 N) and water to remove impurities. Subsequently, the resultant product was annealed at 500℃ for 1 h to get the TNR.

2.2. Synthesis of Cu/TNR

0.49 g of TNR were dispersed in 40 mL of 25% CH_3OH by ultrasonication using a 70 mL pyrex reactor, followed by the addition of a certain amount of $Cu(NO_3)_2$ to the suspension. After sealing the reactor tightly, Ar gas was purged for 30 min to eliminate the dissolved oxygen and subsequently irradiated with a 400 W Hg lamp for 30 min. The resulting mixture was rinsed with water through centrifugation and dried in an oven at 80℃ for 10 h; the product obtained was named as Cu/TNR.

- Hydrogen production measurement

The photocatalytic hydrogen evolution tests of the prepared samples were conducted at ambient temperature and atmospheric pressure in an 80 mL

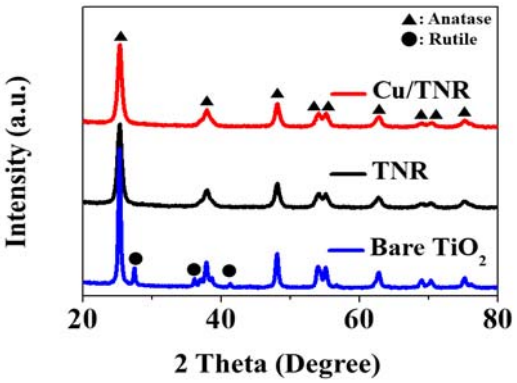

Fig. 1. The XRD spectra of the bare TiO_2, TNR, and Cu/TNR samples.

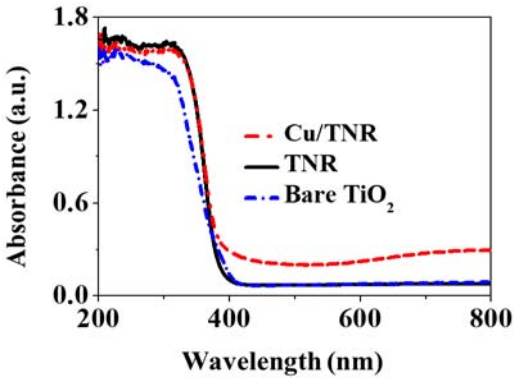

Fig. 2. The UV-vis DRS spectra of the bare TiO_2, TNR, and Cu/TNR samples.

quartz reactor. Briefly, 2 mg of catalyst powder was dispersed into 40 mL of 25% methyl alcohol aqueous solution, and the reactor was then closed securely using a sleeve cover. The dissolved oxygen in the suspension was removed by purging the ultra-pure argon for 30 min. The dispersion was then illuminated with a 300 W xenon lamp (Newport) using AM 1.5G (100 mW/cm) filter under constant stirring. The generated H_2 gas was periodically sampled from the reactor headspace using 500 μL gas-tight syringe (Hamilton). Finally, the H_2 gas produced was quantified by gas chromatography (Shimazu Corp. GC-2010) with a thermal conductivity detector.

• Measurement and analysis

The crystal structure of the prepared catalysts was measured by an X-ray diffractometer (XRD: Rigaku (D/Max-2500)) with Cu Kα radiation (λ = 1.5406 Å). The detailed surface structure was examined on a transmission electron microscope (TEM, Hitachi, HT 7700) and a high-resolution TEM (HRTEM, Titan G2 ChemiSTEM Cs Probe (FEI Company, Netherlands)) equipped with an energy-dispersive X-ray spectrometer (EDS). Ultraviolet-visible diffuse reflectance spectroscopy (UV-vis DRS) studies were carried out on a Shimadzu UV-2600 UV-vis spectrophotometer, using $BaSO_4$ as a reflectance standard. Steady-state photoluminescence (PL) measurements were executed on a Shimadzu RF-6000 spectrofluorophotometer with an excitation wavelength of 300 nm.

3. Results and discussion

The crystal structures of the synthesized catalysts were identified by XRD patterns shown in Fig. 1 Th Measurement e definite peaks at 25.4°, 37.9°, 48.1°, 54.1°, 55.2°, and 62.7° observed in the XRD spectra of the TNR and Cu/TNR are ascribed to the (101), (004), (200), (105), (211), and (204) planes, respectively, and the pattern is well consistent with the standard pattern of anatase TiO_2 (PDF# 01-070-7348). The clear and intense patterns without impurity peaks reflect the crystallinity and purity of the samples. It is also observed that the peaks belonging to Cu did not appear in the XRD patterns of both TNR and Cu/TNR catalysts, possibly due to the high-dispersion and low quantity of Cu in the catalysts (Kadi et al., 2020). Besides, the bare P25 TiO_2 reference sample, as expected, exhibited the patterns of anatase and rutile (Fig. 1), following the previous report (Jiang et al., 2018a).

The light absorption properties of the catalysts were examined using UV−vis DRS studies (Fig. 2). The bare TiO_2 profile illustrated an absorption edge at approximately below 400 nm, referring its UV light

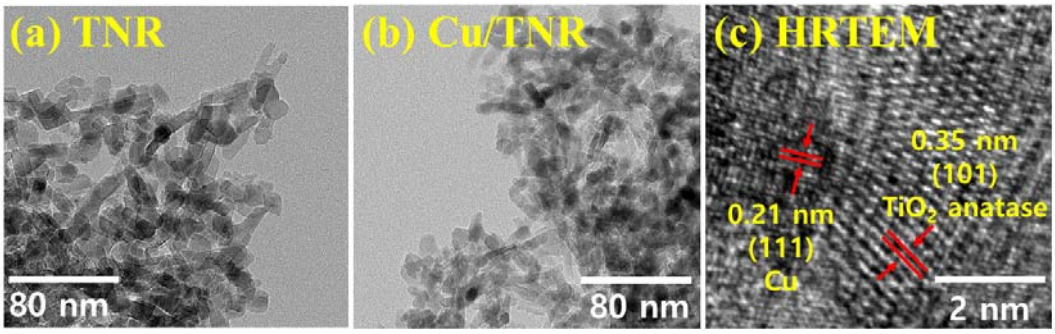

Fig. 3. The TEM images of (a) TNR and (b) Cu/TNR catalysts. (c) The HRTEM image of the Cu/TNR catalyst.

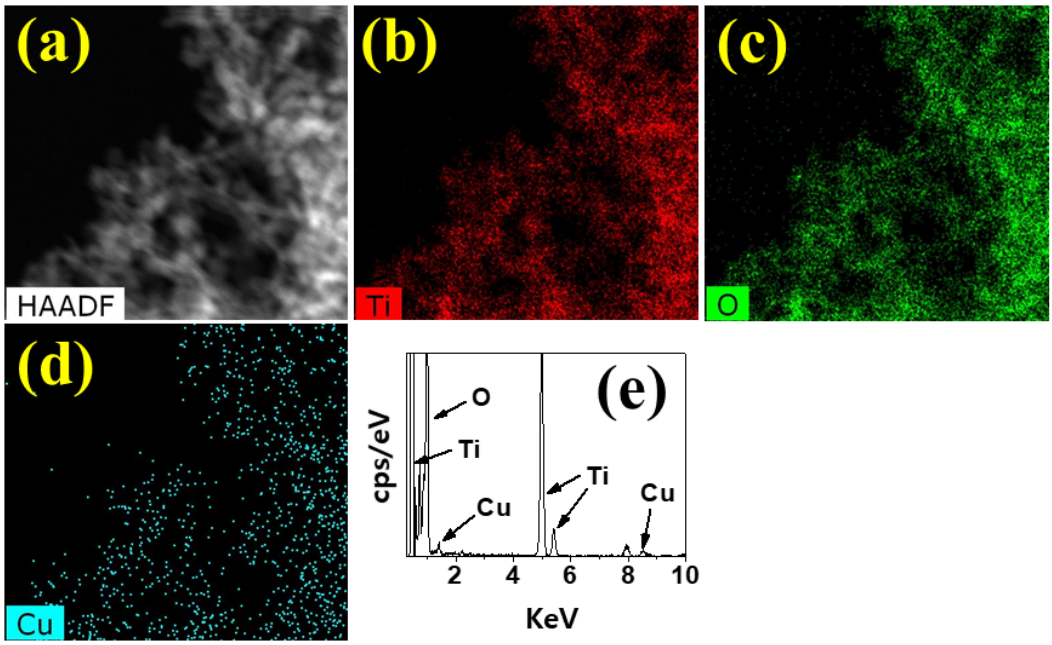

Fig. 4. The elemental mappings (a-d) and EDS profile (e) of the Cu/TNR sample.

response bandgap. The TNR catalyst displayed a slightly altered absorption edge, but with an absorption similar to that of bare TiO_2. Interestingly, the introduction of Cu to the TNR substantially increases the light absorption in the visible range, which could be assigned to the surface plasmon resonance of Cu (DeSario et al., 2017). This indicates that the Cu is successfully loaded onto the surface of TiO_2, which could also serve as direct evidence of the existence of Cu. The improved optical absorption of Cu/TNR catalyst will therefore promote the production of photoinduced charge carriers, which can eventually lead to the improved photocatalytic performance of Cu/TiO_2 for hydrogen production.

TEM examinations explored the morphology and microstructure of the TNR and Cu/TNR samples. As shown in Fig. 3, the TNR sample, different from its bare TiO_2 counterpart with a particle-like morphology, exhibits a rod-like morphology with random sizes. After

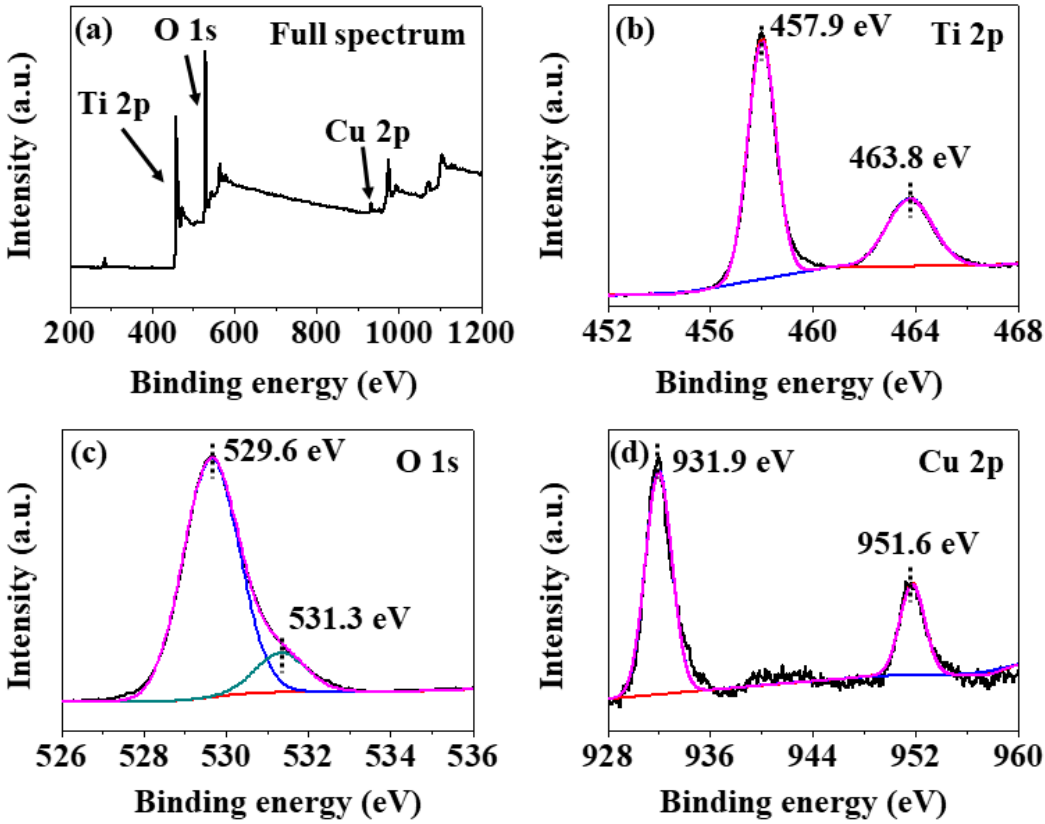

Fig. 5. XPS profiles of the Cu/TNR catalyst. (a) Full spectrum, (b) Ti 2p, (c) O 1s, (d) Cu 2p spectra.

introducing Cu to its surface, TNR retains its rod-like morphology (Rodríguez-Aguado et al., 2019), as shown in Fig. 3b. Although Cu particles cannot be seen in the TEM image, their presence is evidenced by the HRTEM image of Cu/TNR, which shows two distinct lattice fringes with *d*-spacings of 0.35 and 0.21 nm attributed to TiO_2 (101) and metallic Cu (111) planes, respectively (Fernandez-Arias et al., 2020; Wang et al., 2018). Additionally, the elemental mapping images of the Cu/TNR sample (Fig. 5a-d) illustrate the evenly distributed Ti, Cu, and O elements, demonstrating the close integration of the metallic Cu and TNR components. In addition, Ti, O, and Cu were found in the EDS profile of Cu/TNR catalyst (Fig. 5e) further verified the successful decoration of Cu on the TNR surface.

To elucidate the surface elemental composition and valence states of elements in the Cu/TNR catalyst, XPS measurements were performed. The XPS survey spectrum in Fig. 5a reveals that the Cu/TNR catalyst was composed of Ti, O, and Cu elements, reflecting the successful deposition of Cu on the TNR surface, consistent with the findings of the UV-vis DRS and TEM studies. The Ti 2p XPS spectrum of Cu/TNR in Fig. 5b displays two peaks at 457.9 and 463.8 eV attributed to Ti $2p_{3/2}$ and Ti $2p_{1/2}$ spin couple, respectively, indicating the presence of tetravalent Ti ions (Kim and Jo, 2019). Moreover, the O 1s spectrum of Cu/TNR (Fig. 5c) illustrates two peaks representing the lattice oxygen (Ti−O) and surface adsorbed water at 529.6 and 531.3 eV, respectively(Deng et al., 2019). In

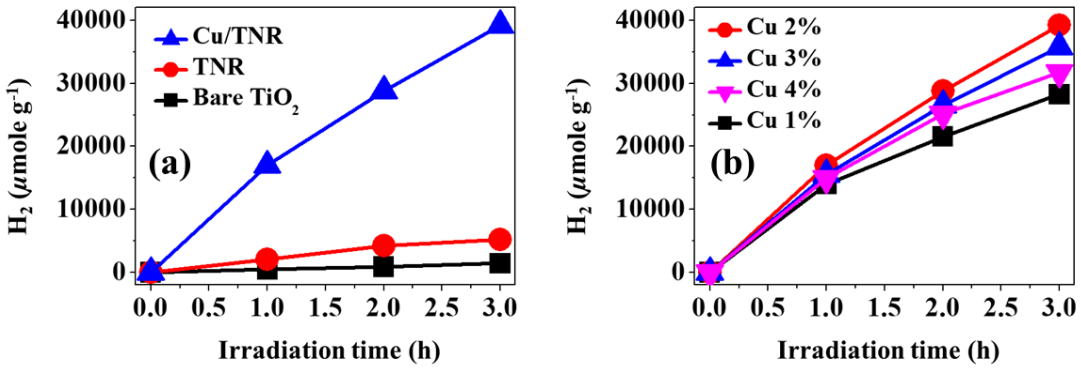

Fig. 6. (a) The hydrogen generation activities of the bare TiO_2, TNR, and Cu/TNR samples. (b) The hydrogen generation activities of the Cu/TNR catalysts with different Cu contents.

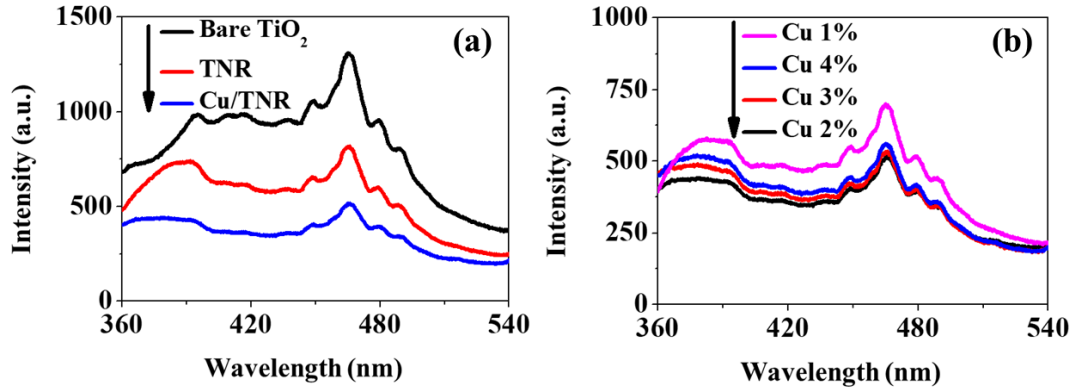

Fig. 7. (a) The PL profiles of the bare TiO_2, TNR, and Cu/TNR samples and (b) The PL profiles of the Cu/TNR samples with different Cu contents.

addition, the Cu spectrum in Fig. 5d displays the peaks related to Cu $2p_{3/2}$ and Cu $2p_{1/2}$ at 931.9 and 951.6 eV, confirming the zero-valence state of Cu in the Cu/TNR (Xu et al., 2019). These findings clearly demonstrated the successful preparation of the metallic Cu loaded TNR catalyst.

Photocatalytic H_2 production activities of the fabricated catalysts were evaluated under simulated solar light with methyl alcohol as a sacrificial reagent to trap photogenerated holes. The variation in H_2 production with illumination time over bare TiO_2, TNR, and Cu/TNR photocatalysts are presented in Fig. 5. After 3 h of light illumination, bare TiO_2 exhibited H_2 generation with a yield of 1,467 μmol/g, whereas TNR displayed a higher H_2 production yield of 5,240 μmol/g, which is more than 3-times higher activity than bare TiO_2. Interestingly, loading Cu onto the surface of TNR greatly enhances photocatalytic activities, resulting in excellent H_2 production yields by all of the Cu/TNR catalysts. It is also observed that with an increase in Cu content, H_2 yields increased first and then declined gradually. In particular, the Cu/TNR catalyst with 2 wt.% of Cu, attained a remarkable H_2 production with a yield of 39,239 μmol/g after 3 h of light illumination,

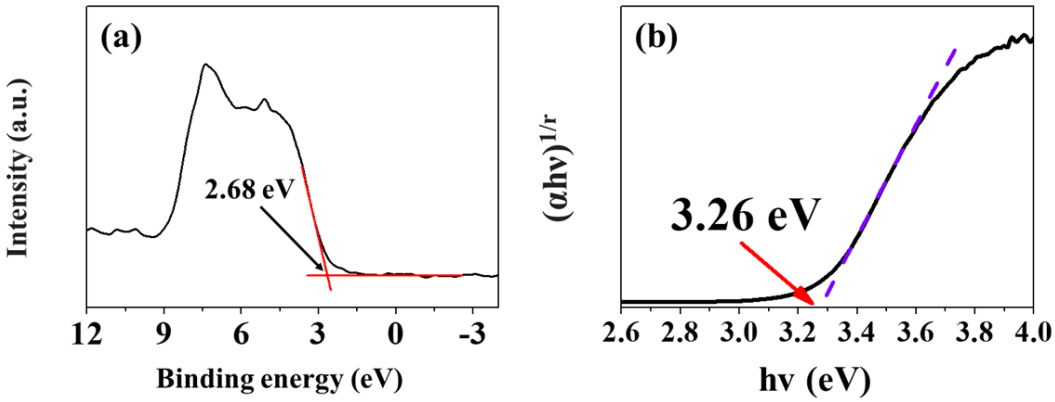

Fig. 8. (a) VB-XPS profile of the TNR (b) Tauc plots to determine the optical band gap of the TNR.

representing 7.4- and 27.7-fold enhancements against TNR and bare TiO_2, respectively. These results suggest that the optimum content of Cu in Cu/TNR catalysts is crucial to achieving the remarkable photocatalytic H_2 efficiency.

The remarkable photocatalytic H_2 evolution of the Cu/TNR catalyst demonstrates the intimate interface between the metallic Cu and TNR components, which in turn facilitates charge transfer and reduces charge recombination. This phenomenon is verified by PL spectra studies. The PL profiles of the bare TiO_2, TNR, and Cu/TNR were illustrated in Fig. 6. In general, a high-intensity PL emission peak reflects a greater chance of electron-hole recombination and lower photocatalytic efficiency (Jo et al., 2019; Jo and Tonda, 2019). Fig. 6a shows that bare TiO_2 displayed the strongest PL emission peak, indicating fast recombination of charge-carrier in the catalyst. Meanwhile, TNR displays a decreased PL emission signal than bare TiO_2, which implies that the recombination of photogenerated charges can be efficiently hampered within the TNR catalyst. Notably, the target Cu/TNR catalyst displayed a substantially quenched PL signal that directly relates to its excellent separation and effectively inhibited recombination of photoexcited charges compared to other reference catalysts, bare TiO_2 and TNR. These results are consistent with the results of the photocatalytic hydrogen production yields of the catalysts. Furthermore, PL studies were also applied to examine the impact of Cu amount on the photocatalytic properties of the Cu/TNR catalysts. As expected, the Cu/TNR catalyst with 2 wt.% of Cu demonstrated the lowest PL emission intensity among the catalysts with different Cu contents (Fig. 6b), in accordance with the H_2 production activities.

The PL results discussed above indeed concluded that the remarkable H_2 evolution activity of the Cu/TNR was attributed primarily to the intimate interface between metallic Cu and TNR components, where the photoexcited charge carriers could be efficiently separated. In addition to this factor, the effective optical absorption of the Cu/TNR catalyst was another important factor that significantly influenced the photocatalytic H_2 evolution performance of the Cu/TNR, as verified by the UV-vis DRS studies discussed above. In addition, the valence band XPS (VB-XPS) and the Tauc plots were applied to explore the band edge potentials of the present catalyst. Fig. 7a displays the VB-XPS profile of the TNR from which the VB potential was estimated to be 2.68 eV. The bandgap of the catalyst determined from the Tauc plot was 3.26

Table 1. Comparison of photocatalytic activity in hydrogen production

Photocatalyst	Co-catalyst	Light source (light intensity)	Sacrificial solution	H_2 production rate (μmol/g/h)	Quantum efficiency (%)	Reference
Cu/TNR	Cu	300 W Xe lamp (100 mW/cm^2)	25% methanol	13,079	18.75	This work
Cu/TiO_2	Cu	300 W Xe lamp (80.0 mW/cm^2)	10% methanol	2,800	4.3	(Tian et al., 2014)
$Cu(OH)_2/TiO_2$	$Cu(OH)_2$	4×3W UV-LED (80.0 mW/cm^2)	0.09 M ethylene glycol	3,418	13.9	(Yu and Ran, 2011)
Cu_2O/TiO_2	Cu_2O	300 W Xe lamp (80.0 mW/cm^2)	20% methanol	1,523	7.05	(Liu et al., 2015)
Cu-TiO_2 nanowire	Cu	4×3W UV-LED (80.0 mW/cm^2)	25% methanol	5,104	17.2	(Xiao et al., 2015)

eV. By combining these results, the conduction band (CB) potential of the catalyst was measured as −0.58 eV.

Based on the above experimental results, the photocatalytic mechanism for the remarkable H_2 evolution activity of the developed catalyst was presented schematically in Fig. 8 and explained as follows. Under the applied light illumination, the catalyst can absorb the photons and be excited to generate electrons (e^-) and holes (h^+) in the CB and the VB, respectively. The excited e^- in the CB of TNR is readily captured by the metallic Cu owing to its extraordinary electron trapping properties (Li et al., 2019a), which results in an e^- accumulation on the metallic Cu surface. Meanwhile, the holes at the VB of TNR can react with methanol (sacrificial reagent), which results in reduced recombination of photoexcited e^- and h^+. After being captured by the metallic Cu, the photogenerated e^- will further reduce the protons in the aqueous solution to produce H_2.

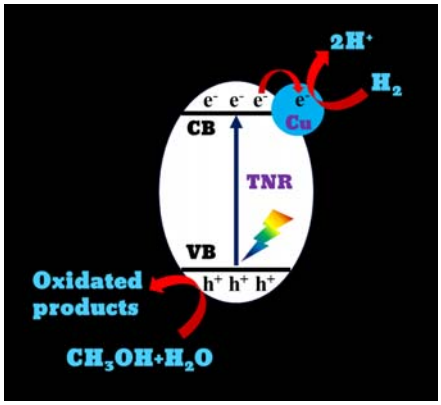

Fig. 9. Schematic illustration of the proposed mechanism for hydrogen production in the Cu/TNR photocatalyst.

4. Conclusions

In this study, an efficient Cu/TNR photocatalyst was fabricated via a facile hydrothermal method followed by a photodeposition technique. The results of different characterization techniques confirmed the successful formation of the Cu/TNR photocatalyst. Markedly, the fabricated Cu/TNR catalyst with optimum Cu content, achieved a remarkable production of H_2 with a yield of 39,239 μmol/g after 3 h of solar light illumination, representing 7.4- and 27.7-fold improvements against TNR and commercial P25, respectively. The notably improved light absorption of the Cu/TNR catalyst, which helps to produce more photoexcited charges, was crucial to the improvement of the H_2 evolution activity. In addition, the excellent separation of photoexcited electron-hole pairs is another key factor that significantly influenced the H_2 evolution of the target

Cu/TNR catalyst. This study, therefore, gives an insight into the fabrication of low-cost transition metal-loaded TiO_2 photocatalysts for photocatalytic green energy production.

Acknowledgments

This research was supported by Kyungpook National University Development Project Research Fund, 2018.

REFERENCE

Deng, Y., Li, S., Li, X., Wang, R., Li, X., 2019, Green low-temperature-solution-processed in situ HI modified TiO_2/SnO_2 bilayer for efficient and stable planar perovskite solar cells build at ambient air conditions, Electrochim. Acta, 326, 134924.

DeSario, P. A., Pietron, J. J., Brintlinger, T. H., McEntee, M., Parker, J. F., Baturina, O., Stroud, R. M., Rolison, D. R., 2017, Oxidation-stable plasmonic copper nanoparticles in photocatalytic TiO_2 nanoarchitectures, Nanoscale, 9, 11720-11729.

Fernandez-Arias, M., Boutinguiza, M., Del Val, J., Riveiro, A., Rodriguez, D., Arias-Gonzalez, F., Gil, J., Pou, J., 2020, Fabrication and deposition of copper and copper oxide nanoparticles by laser ablation in open air, Nanomaterials, 10, 300.

Ganguly, P., Harb, M., Cao, Z., Cavallo, L., Breen, A., Dervin, S., Dionysiou, D. D., Pillai, S. C., 2019, 2D nanomaterials for photocatalytic hydrogen production, ACS Energy Lett., 4, 1687-1709.

Gao, C., Wei, T., Zhang, Y., Song, X., Huan, Y., Liu, H., Zhao, M., Yu, J., Chen, X., 2019, A Photoresponsive rutile TiO_2 Heterojunction with enhanced electron-hole separation for high-performance hydrogen evolution, Adv. Mater., 31, 1806596.

Hu, Q., Li, G., Lan, H., Li, J., Hu, B., Guo, W., Huang, J., Huang, X., 2019, Facile coengineering of oxygen defects and highly active {110} facets in TiO_2 nanorods for efficient water splitting, Cryst. Growth Des., 19, 1680-1688.

Jiang, X., Manawan, M., Feng, T., Qian, R., Zhao, T., Zhou, G., Kong, F., Wang, Q., Dai, S., Pan, J. H., 2018a. Anatase and rutile in evonik aeroxide P25: Heterojunctioned or individual nanoparticles?, Catal. Today, 300, 12-17.

Jiang, Y., Ning, H., Tian, C., Jiang, B., Li, Q., Yan, H., Zhang, X., Wang, J., Jing, L., Fu, H., 2018b, Single -crystal TiO_2 nanorods assembly for efficient and stable cocatalyst-free photocatalytic hydrogen evolution, Appl. Catal. B, 229, 1-7.

Jin, Y. J., Jo, W. K., 2018, Upgraded organic vapor treatment and hydrogen generation using low-cost metal/1D black titania nanocomposites under simulated solar irradiation, J. Ind. Eng. Chem., 66, 318-324.

Jo, W. K., Kim, Y. G., Tonda, S., 2018b, Hierarchical flower -like NiAl-layered double hydroxide microspheres encapsulated with black Cu-doped TiO_2 nanoparticles: Highly efficient visible-light-driven composite photocatalysts for environmental remediation., J. Hazard. Mater, 357, 19-29.

Jo, W. K., Kumar, S., Tonda, S., 2019, N-doped C dot/CoAl-layered double hydroxide/g-C_3N_4 hybrid composites for efficient and selective solar-driven conversion of CO_2 into CH_4, Compos. Part B. Eng., 176, 107212.

Jo, W. K., Kumar, S., Yadav, P., Tonda, S., 2018a, In situ phase transformation synthesis of unique Janus Ag_2O/Ag_2CO_3 heterojunction photocatalyst with improved photocatalytic properties, Appl. Surf. Sci., 445, 555-562.

Jo, W. K., Moru, S., Tonda, S., 2020, Magnetically responsive $SnFe_2O_4$/g-C_3N_4 hybrid photocatalysts with remarkable visible-light-induced performance for degradation of environmentally hazardous substances and sustainable hydrogen production, Appl. Surf. Sci., 506, 144939.

Jo, W. K., Tonda, S., 2019, Novel CoAl-LDH/g-C_3N_4/RGO ternary heterojunction with notable 2D/2D/2D configuration for highly efficient visible-light-induced photocatalytic elimination of dye and antibiotic pollutants, J. Hazard. Mater., 368, 778-787.

Kadi, M. W., Mohamed, R. M., Ismail, A. A., 2020, Uniform dispersion of CuO nanoparticles on mesoporous TiO_2 networks promotes visible light photocatalysis, Ceram. Int., 46, 8819-8826.

Khatun, N., Tiwari, S., Lal, J., Tseng, C. M., Liu, S. W., Biring, S., Sen, S., 2018, Stabilization of anatase phase

by uncompensated Ga-V co-doping in TiO_2: A structural phase transition, grain growth and optical property study, Ceram. Int., 44, 22445-22455.

Kim, D. J., Jo, W. K., 2018, Mitigation of harmful indoor organic vapors using plug-flow unit coated with 2D g-C_3N_4 and metallic Cu dual-incorporated 1D titania heterostructure. Chemosphere 202, 184-190.

Kim, D. J., Jo, W. K., 2019, Sustainable treatment of harmful dyeing industry pollutants using $SrZnTiO_3$/g-C_3N_4 heterostructure with a light source-dependent charge transfer mechanism, Appl. Catal. B, 242, 171-177.

Koltsakidou, A., Antonopoulou, M., Epsilonvgenidou, E., Konstantinou, I., Giannakas, A. E., Papadaki, M., Bikiaris, D., Lambropoulou, D. A., 2017, Photocatalytical removal of fluorouracil using TiO_2-P25 and N/S doped TiO_2 catalysts: A kinetic and mechanistic study, Sci. Total Environ., 578, 257-267.

Kumaravel, V., Mathew, S., Bartlett, J., Pillai, S. C., 2019, Photocatalytic hydrogen production using metal doped TiO_2: A review of recent advances, Appl. Catal. B, 244, 1021-1064.

Lee, B. H., Park, S., Kim, M., Sinha, A. K., Lee, S. C., Jung, E., Chang, W. J., Lee, K. S., Kim, J. H., Cho, S. P., Kim, H., Nam, K. T., Hyeon, T., 2019, Reversible and cooperative photoactivation of single-atom Cu/TiO_2 photocatalysts. Nat. Mater., 18(6), 620-626.

Li, G., Huang, J., Deng, Z., Chen, J., Huang, Q., Liu, Z., Guo, W., Cao, R., 2019a, Highly active photocatalyst of CuO_x modified TiO_2 arrays for hydrogen generation, Cryst. Growth Des., 19, 5784-5790.

Li, Q., Zhao, T., Li, M., Li, W., Yang, B., Qin, D., Lv, K., Wang, X., Wu, L., Wu, X., Sun, J., 2019b, One-step construction of Pickering emulsion via commercial TiO_2 nanoparticles for photocatalytic dye degradation. Appl. Catal. B, 249, 1-8.

Liu, Y., Zhang, B., Luo, L., Chen, X., Wang, Z., Wu, E., Su, D., Huang, W., 2015, TiO_2 /Cu_2O Core/Ultrathin Shell Nanorods as Efficient and Stable Photocatalysts for Water Reduction. Angew. Chem. Int. Ed., 54, 15260-15265.

Park, J., Lim, J., Park, Y., Han, D. S., Shon, H. K., Hoffmann, M. R., Park, H., 2020, In situ-generated reactive oxygen species in precharged titania and tungsten trioxide composite catalyst membrane filters: Application to as(III) oxidation in the absence of irradiation, Environ. Sci. Technol., 54, 9601-9608.

Peng, C., Wei, P., Li, X., Liu, Y., Cao, Y., Wang, H., Yu, H., Peng, F., Zhang, L., Zhang, B., Lv, K., 2018, High efficiency photocatalytic hydrogen production over ternary Cu/TiO_2@$Ti_3C_2T_x$ enabled by low-work -function 2D titanium carbide, Nano Energy, 53, 97-107.

Rodríguez-Aguado, E., Infantes-Molina, A., Talon, A., Storaro, L., León-Reina, L., Rodríguez-Castellón, E., Moretti, E., 2019, Au nanoparticles supported on nanorod-like TiO_2 as catalysts in the CO-PROX reaction under dark and light irradiation: Effect of acidic and alkaline synthesis conditions, Int. J. Hydrog. Energy, 44, 923-936.

Seetharaman, A., Sivasubramanian, D., Gandhiraj, V., Soma, V. R., 2017, Tunable manosecond and femtosecond nonlinear optical properties of C−N− S-Doped TiO_2 nanoparticles, J. Phys. Chem. C, 121, 24192-24205.

Sharma, A., Lee, B. K., 2017, Photocatalytic reduction of carbon dioxide to methanol using nickel-loaded TiO_2 supported on activated carbon fiber, Catal. Today, 298, 158-167.

Singh, R., Dutta, S., 2018, A Review on H_2 production through photocatalytic reactions using TiO_2/TiO_2 -assisted catalysts, Fuel, 220, 607-620.

Sorcar, S., Hwang, Y., Lee, J., Kim, H., Grimes, K. M., Grimes, C. A., Jung, J. W., Cho, C. H., Majima, T., Hoffmann, M. R., In, S. I., 2019, CO_2, water, and sunlight to hydrocarbon fuels: a sustained sunlight to fuel (Joule-to-Joule) photoconversion efficiency of 1%, Energy Environ. Sci., 12, 2685-2696.

Sorcar, S., Thompson, J., Hwang, Y., Park, Y. H., Majima, T., Grimes, C. A., Durrant, J. R., In, S. I., 2018, High-rate solar-light photoconversion of CO_2 to fuel: controllable transformation from C_1 to C_2 products, Energy Environ. Sci., 11, 3183-3193.

Tian, H., Zhang, X. L., Scott, J., Ng, C., Amal, R., 2014, TiO_2-supported copper nanoparticles prepared via ion exchange for photocatalytic hydrogen production, J. Mater. Chem. A, 2, 6432-6438.

Wang, X., Xia, R., Muhire, E., Jiang, S., Huo, X., Gao, M., 2018, Highly enhanced photocatalytic performance of TiO_2 nanosheets through constructing TiO_2/TiO_2 quantum dots homojunction, Appl. Surf. Sci., 459, 9-15.

Wei, T., Zhu, Y., Wu, Y., An, X., Liu, L. M., 2019, Effect of single-atom cocatalysts on the activity of faceted TiO_2 photocatalysts, Langmuir, 35, 391-397.

Xiao, S., Liu, P., Zhu, W., Li, G., Zhang, D., Li, H., 2015, Copper nanowires: A Substitute for noble metals to enhance photocatalytic H_2 generation, Nano Lett., 15, 4853-4858.

Xu, L., Li, J., Sun, H., Guo, X., Xu, J., Zhang, H., Zhang, X., 2019, In situ growth of Cu_2O/CuO nanosheets on Cu coating carbon cloths as a binder-free electrode for asymmetric supercapacitors, Front. Chem., 7, 420.

Yu, J., Ran, J., 2011, Facile preparation and enhanced photocatalytic H_2-production activity of $Cu(OH)_2$ cluster modified TiO_2, Energy Environ. Sci., 4, 1364.

Yuan, Y. J., Chen, D., Yu, Z. T., Zou, Z. G., 2018, Cadmium sulfide-based nanomaterials for photocatalytic hydrogen production, J. Mater. Chem. A, 6, 11606-11630.

Zhang, J., Yu, Z., Gao, Z., Ge, H., Zhao, S., Chen, C., Chen, S., Tong, X., Wang, M., Zheng, Z., Qin, Y., 2017, Porous TiO_2 nanotubes with spatially separated platinum and CoO_x cocatalysts produced by atomic layer deposition for photocatalytic hydrogen production, Angew. Chem. Int. Ed., 56, 816-820.

• Doctor's course. Dong-Jin Kim
Department of Environmental Engineering, Kyungpook National University
eastcamp@knu.ac.kr
• Research professor. Surendar Tonda
Department of Environmental Engineering, Kyungpook National University
surendar.t86@gmail.com
• Professor. Wan-Kuen Jo
Department of Environmental Engineering, Kyungpook National University
wkjo@knu.ac.kr